17. Unified method for analysis of laterally loaded piles in clay

W. R. SULLIVAN, MSCE (recently Staff Engineer, ARMAC Engineers, Inc., Tampa, Florida, now Geotechnical Engineer, Golder Associates, Atlanta, Georgia), L. C. REESE, PE, PhD, (T. U. Taylor Professor of Civil Engineering and Associate Dean, College of Engineering, The University of Texas at Austin) and C. W. FENSKE, PE, MSCE (Manager of Engineering, McClelland Engineers, Inc., Houston, Texas)

The behaviour of a pile under lateral loading is obtained by solving an equation by digital computer. The equation includes a term at each depth for the soil modulus. The soil response is given by a family of curves giving soil resistance as a function of pile deflexion (p–y curves). The soil moduli are secants to the p–y curves and can vary in any arbitrary manner with depth. Two major experimental programmes have been performed in the field on full-sized, instrumented piles in clay that is submerged. One series of experiments was performed in soft to medium clay and the other in stiff clay. Results from these two studies have been reanalysed and a unified method has been proposed for predicting p–y curves for clay. The properties of the clay are given by the undrained shear strength, the submerged unit weight, and the shape of the stress–strain curve. The method can treat the cases of short term and repeated loading and can be applied to the analysis of piles of any geometry, stiffness, and pile head fixity. Predictions of pile behaviour were made using the unified method and were compared with results from experiments. The unified method has been shown to be an acceptable approach. A number of practical problems can be attacked with considerable success. Agreement between predictions with the analytical method and experimental results are good or show the analytical method to be somewhat conservative.

INTRODUCTION

While axially loaded piles frequently may be designed satisfactorily by simple static methods, the design procedure for laterally loaded piles is more complex, involving the solution of a fourth-order differential equation. The solution must ensure that conditions of equilibrium and compatibility are satisfied. The problem of laterally loaded piles is further complicated because of the non-linear soil response.

2. The differential equation to be solved, as derived from conventional beam theory,[1] is

$$EI\frac{d^4y}{dx^4} + P_x\frac{d^2y}{dx^2} - p = 0 \qquad (1)$$

where EI is flexural rigidity of pile, y is deflexion of pile, x is length along pile, P_x is axial load, and p is soil reaction per unit length. Equation (1) may be solved conveniently by a digital computer;[2] however, non-dimensional methods may sometimes be employed to yield an acceptable solution.[3] Both methods of solution give all the necessary design information, including the moment, deflexion and shear at desired lengths along the pile.

SOIL RESPONSE

3. The approach to solving the problem of laterally loaded piles is based on the assumption attributed to Winkler.[4] The soil surrounding a pile is depicted as a set of non-linear elastic springs, and the Winkler assumption states that each spring acts independently. The depression of one spring has no effect on an adjacent spring. It is obvious that the Winkler assumption is not valid for soils; however, the errors involved in the use of the assumption are relatively small.

4. It is convenient to think of the soil response in terms of a p–y curve. Fig. 1 defines the concept. Part (a) of the figure shows the depth at which the soil behaviour is considered. Part (b) depicts the probable earth pressure distribution prior to any lateral loading. Part (c) shows a possible earth pressure distribution after the section under consideration has deflected a distance y_1. As the deflexion increases, the soil resistance on the section of the shaft changes. A possible family of p–y curves is shown in Fig. 2; each curve represents the soil behaviour at a different depth.

5. For convenience in solving equation (1), a secant modulus of soil reaction, E_s, is often used (Fig. 3):

$$E_s = -p/y \qquad (2)$$

As may be understood from Figs 2 and 3, E_s can vary in an arbitrary manner with depth and with deflexion.

6. Two major experimental programmes have been carried out on full-sized, instrumented piles that were installed in clays below a water surface. The two programmes have led to recommendations for the prediction of families of p–y curves. Brief descriptions of the programmes and their results are presented in the following sections.

EXPERIMENTAL PROGRAMME WITH PILES IN SOFT CLAY

7. Matlock[4] performed lateral load tests employing a steel pipe pile 325 mm in diameter and 12.8 m in length. It was driven into clays near Lake Austin that had a shear strength of about 38 kPa. The pile was recovered, taken to Sabine Pass, Texas, and driven into clay with a shear strength that averaged about 14 kPa in the significant upper zone.

8. Families of bending moment curves were obtained from electrical resistance strain gauges that were attached to the interior of the pile. Sets of curves were obtained for short term static loading and other sets were obtained for cyclic loading. The effects of soil creep were minimized in the short term testing. In the cyclic tests, a load of a given magnitude was repeated until the deflexions and bending moment reached an equilibrium condition. The data were analysed and experimental p–y curves were obtained.[5] Principles of mechanics were employed to the extent possible and equations were developed for prediction of p–y curves on the basis of soil properties, pile geometry, and nature of loading.

9. Matlock[4] recommended the following procedure for p–y curves for soft clay for short term static loading (Fig. 4 (a)).

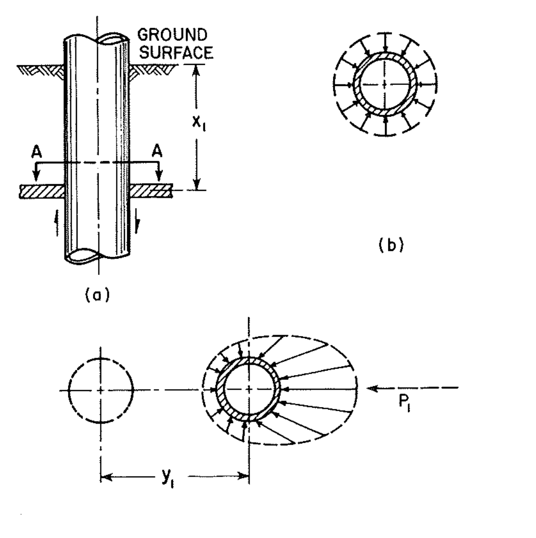

Fig. 1. Graphical definition of p and y: (a) pile elevation; (b) view AA – earth pressure distribution prior to lateral loading; (c) view AA – earth pressure distribution after lateral loading

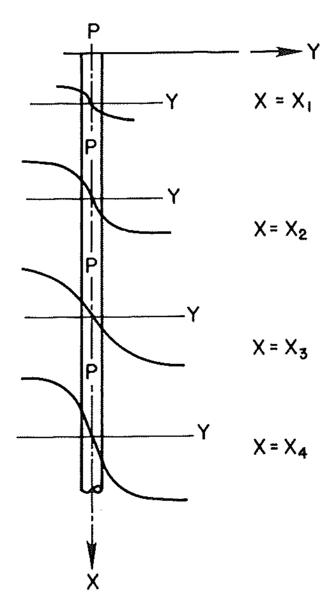

Fig. 2. p–y curves

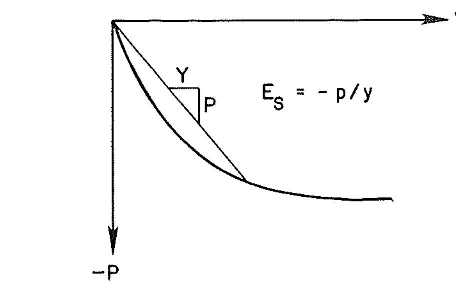

Fig. 3. Illustration of the secant modulus

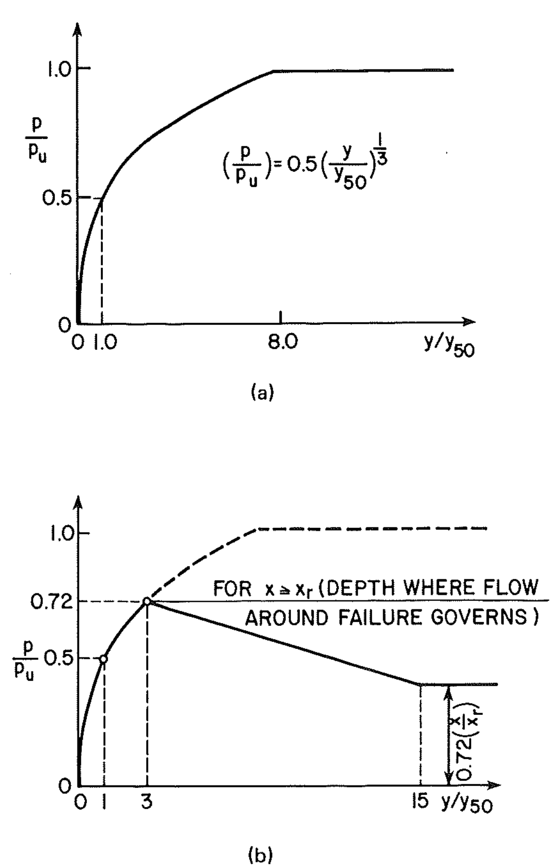

Fig. 4. Characteristic shapes of p–y curves for soft clay below the water surface: (a) short term static loading; (b) cyclic loading

(a) Obtain the best possible estimate of the undrained shear strength and effective unit weight with depth. Also obtain the value of ϵ_{50}, the strain corresponding to one half the maximum principal stress difference. If no values of ϵ_{50} are available, typical values suggested by Skempton[6] are given in Table 1.

(b) Compute the ultimate soil resistance per unit length of the pile, p_u; use the smaller of the values given by the equations below:

$$p_u = \left\{3 + \frac{\bar{\gamma}}{s_u}x + \frac{0.5}{b}x\right\} s_u b \qquad (3)$$

$$p_u = 9\, s_u b \qquad (4)$$

where $\bar{\gamma}$ is average effective unit weight from ground surface to depth of p–y curve, x is distance from ground surface to depth of p–y curve, s_u is undrained shear strength at depth x, and b is width of pile. The value of p_u is computed at each depth where a p–y curve is desired, based on shear strength at that depth.

(c) Compute the deflexion, y_{50}, at one half the ultimate soil resistance from the following equation:

$$y_{50} = 2.5\, \epsilon_{50} b \qquad (5)$$

(d) Points describing the p–y curve are now computed from the following relationship:

$$p/p_u = 0.5\, (y/y_{50})^{1/3} \qquad (6)$$

The value of p remains constant at p_u beyond a y value of $8y_{50}$.

10. The following procedure is for cyclic loading (Fig. 4(b)).

(a) Construct the p–y curve in the same manner as for short term static loading for values of p less than $0.72p_u$.

(b) Solve equations (3) and (4) simultaneously to find the depth, x_r, where the transition occurs. If the unit weight and shear strength are constant in the upper zone, then

$$x_r = \frac{6 s_u b}{\gamma b + 0.5 s_u} \qquad (7)$$

If the unit weight and shear stregth vary with depth, the value of x_r should be computed with the soil properties at the depth where the p–y curve is desired.

(c) If the depth of the p–y curve is greater than or equal to x_r, then $p = 0.72p_u$ for all values of y greater than $3y_{50}$.

(d) If the depth to the p–y curve is less than x_r, then the value of p decreases from $0.72p_u$ at $y = 3y_{50}$ to the value given by the following expression at $y = 15y_{50}$:

Table 1. Suggested values of ϵ_{50} for soft clay

Consistency of clay	ϵ_{50}
Soft	0.020
Medium	0.010
Stiff	0.005

NOTATION

A	coefficient used to define the shape of the p–y curve for the unified clay criteria
A_c, A_s	empirical parameters for developing p–y curves for stiff clay below water surface
b	width of pile
EI	flexural rigidity of pile
E_s	secant modulus of soil reaction
E_{sc}	slope of portion of p–y curve for stiff clay below water surface
E_{si}	slope of initial portion of p–y curve for stiff clay below water surface
E_{ss}	slope of portion of p–y curve for stiff clay below water surface
$(E_s)_{max}$	limiting maximum value of soil modulus on p–y curve for unified clay criteria
F	coefficient used to define deterioration of soil resistance at large deformations for short term static loading for the unified clay criteria
k	coefficient of horizontal subgrade modulus
k_c	coefficient of initial soil modulus for cyclic loading for stiff clay below water surface
k_s	coefficient of initial soil modulus for short term static loading for stiff clay below water surface
LI	liquidity index
N_p	soil resistance factor employed in development of unified clay criteria for stiff clay below water surface
PI	plasticity index
P_x	axial load on pile
p	soil reaction per unit length of pile
p_R	peak cyclic resistance on p–y curve
p_u	ultimate soil resistance per unit length of pile
p_{CR}	residual soil resistance on cyclic p–y curve for unified clay criteria
p_{offset}	quantity used in developing p–y curve for stiff clay below water surface
s_u	undrained shear strength at depth x
$(s_u)_{avg}$	average undrained soil shear strength above depth x
w_L	liquid limit
x	length along pile or distance from ground surface to depth at which p–y curve applies
x_r	depth below ground surface to transition in ultimate soil resistance equations
y	deflexion of pile
y_p	value of y at transition point on p–y curve for cyclic loading for stiff clay below water surface
y_{50}	deflexion at one half the ultimate soil resistance
γ	effective unit weight of soil
$\bar{\gamma}$	average effective unit weight from ground surface to depth at which p–y curve applies
ϵ_{50}	strain corresponding to one half the maximum principal stress difference

$$p = 0.72p_u\,(x/x_r) \tag{8}$$

The value of p remains constant at the value given by equation (8) beyond a y value of $15y_{50}$.

11. For determining the shear strength of the soil required in the p–y construction, Matlock[4] recommended the following tests in order of preference:

(a) in-situ vane shear tests with parallel sampling for soil identification;
(b) unconsolidated undrained triaxial compression tests having a confining stress equal to the overburden pressure with the shear strength being defined as half the total maximum principal stress difference;
(c) miniature vane tests of samples in tubes;
(d) unconfined compression tests.

12. Tests must also be performed to determine the unit weight of the soil.

EXPERIMENTAL PROGRAMME WITH PILES IN STIFF CLAY

13. Reese et al.[7] performed lateral load tests employing steel pipe piles 610 mm in outside diameter and 15.2 m in length. The piles were driven into stiff clay at a site near Manor, Texas. The clay had an undrained shear strength ranging from about 96 kPa at the ground surface to about 290 kPa at a depth of 3.66 m.

14. Experimental and analytical procedures were followed that were similar to those employed by Matlock.[4] The following procedure was recommended for p–y curves for stiff clay for short term static loading (Fig. 5).

(a) Obtain the best possible estimate of the undrained shear strength and effective unit weight with depth. If no values of ϵ_{50} are available, use values from Table 2.

Table 2. Recommended value of ϵ_{50} for stiff clays

	Average undrained shear strength, kPa		
	50–100	100–200	200–400
ϵ_{50}	0.007	0.005	0.004

(b) Compute the average undrained soil shear strength, $(s_u)_{avg}$, over the depth x.
(c) Compute the ultimate soil resistance; use the smaller of the values given by the equations below:

$$p_u = \left\{2 + \frac{\gamma}{(s_u)_{avg}}\,x + \frac{2.83}{b}\,x\right\}(s_u)_{avg}b \tag{9}$$

$$p_u = 11s_u b \tag{10}$$

(d) Establish the initial straight-line portion of the p–y curve,

$$p = kxy = E_{si}y \tag{11}$$

Use the appropriate value of k_s or k_c from Table 3.
(e) Compute the following:

$$y_{50} = \epsilon_{50}b \tag{12}$$

(f) Choose an appropriate value of A_s from Fig. 6 for the particular non-dimensional depth.
(g) Establish the first parabolic portion of the p–y curve,

$$p = 0.5p_u(y/y_{50})^{0.5} \tag{13}$$

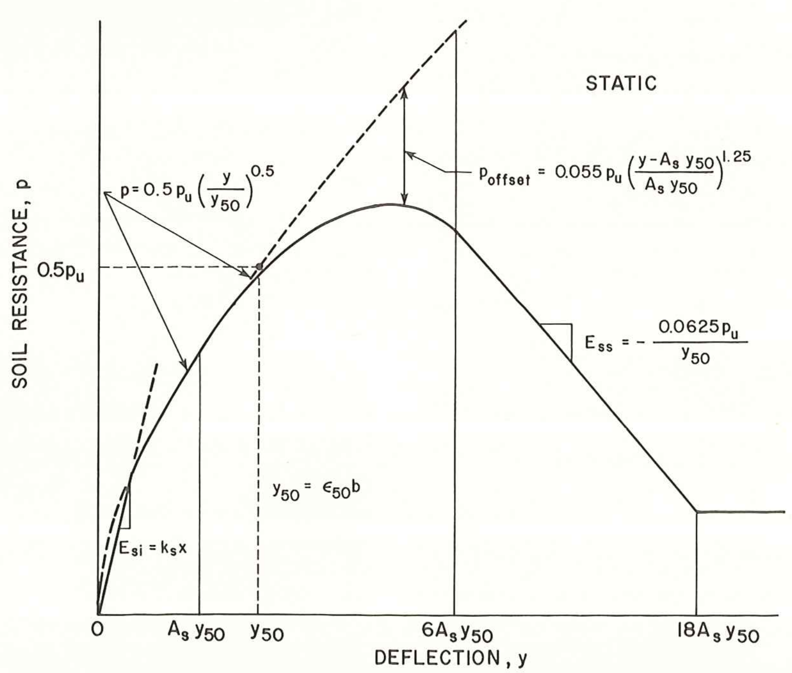

Fig. 5. Characteristic shape of p–y curve for static loading in stiff clay below the water surface

Equation (13) should define the portion of the p–y curve from the point of the intersection with equation (11) to a point where $y = A_s y_{50}$ (see note in paragraph 15).
(h) Establish the second parabolic portion of the p-y curve,

$$p = 0.5p_u(y/y_{50})^{0.5} - 0.055p_u\left\{\frac{y}{A_s y_{50}} - 1\right\}^{1.25} \tag{14}$$

Equation (14) should define the portion of the p–y curve from the point where $y = A_s y_{50}$ to a point where $y = 6A_s y_{50}$ (see note in paragraph 15).
(i) Establish the next straight-line portion of the p–y curve,

$$p = 0.5p_u(6A_s)^{0.5} - 0.411p_u - 0.0625\,(p_u/y_{50})(y - 6A_s y_{50}) \tag{15}$$

Equation (15) should define the portion of the p–y curve from the point where $y = 6A_s y_{50}$ to a point where $y = 18A_s y_{50}$ (see note in paragraph 15).
(j) Establish the final straight-line portion of the p–y curve,

$$p = 0.5p_u(6A_s)^{0.5} - 0.411p_u - 0.75p_u A_s \tag{16}$$

Equation (16) should define the portion of the p–y curve from the point where $y = 18A_s y_{50}$ and for all larger values of y (see following note).

15. Note: The step-by-step procedure is outlined, and Fig. 5 is drawn, as if there is an intersection between equations (11) and (13). However, there may be no intersection of equation (11) with any of the other equations defining the p–y curve. Equation (11) defines the p–y curve until it intersects with one of the other equations or, if no intersection occurs, equation (11) defines the complete p–y curve.

16. The following procedure is for cyclic loading (Fig. 7).

(a) Use step (a) as for the static case.
(b) Use step (b) as for the static case.
(c) Use step (c) as for the static case.
(d) Choose the appropriate value of A_c from Fig. 6 for the particular non-dimensional depth.

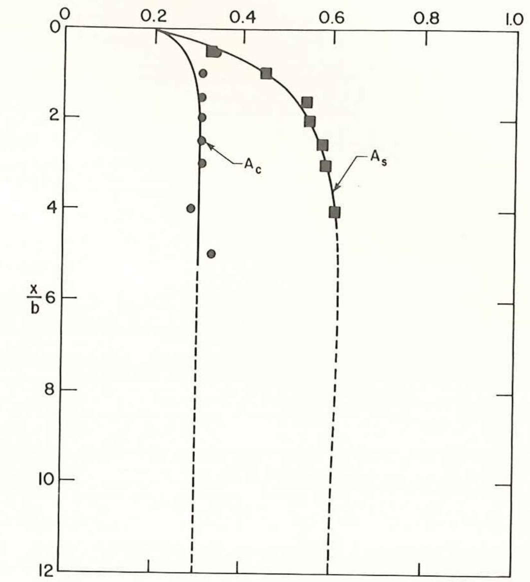

Fig. 6. Values of parameters A_s and A_c

(e) Use step (e) as for the static case.
(f) Compute the following:

$$y_{50} = \epsilon_{50}b \tag{17}$$

$$y_p = 4.14A_s y_{50} \tag{18}$$

(g) Establish the parabolic portion of the p–y curve,

$$p = A_c p_u\left(1 - \left\{\frac{y - 0.45y_p}{0.45y_p}\right\}^{2.5}\right) \tag{19}$$

Equation (19) should define the portion of the p–y curve from the point of the intersection with equation (11) to where $y = 0.6y_p$ (see note in paragraph 17).
(h) Establish the next straight-line portion of the p–y curve,

$$p = 0.936A_c p_u - 0.085\,(p_u/y_{50})(y - 0.6y_p) \tag{20}$$

Equation (20) should define the portion of the p–y curve from the point where $y = 0.6y_p$ to the point where $y = 1.8y_p$ (see note in paragraph 17).

Table 3. Recommended values of k for stiff clays

	Average undrained shear strength,* kPa		
	50–100	100–200	200–400
k_s (static), MN/m^3	135	270	540
k_c (cyclic), MN/m^3	55	110	220

*The average shear strength should be computed from the shear strength of the soil to a depth of 5 pile diameters. It should be defined as half the total maximum principal stress difference in an unconsolidated undrained triaxial test.

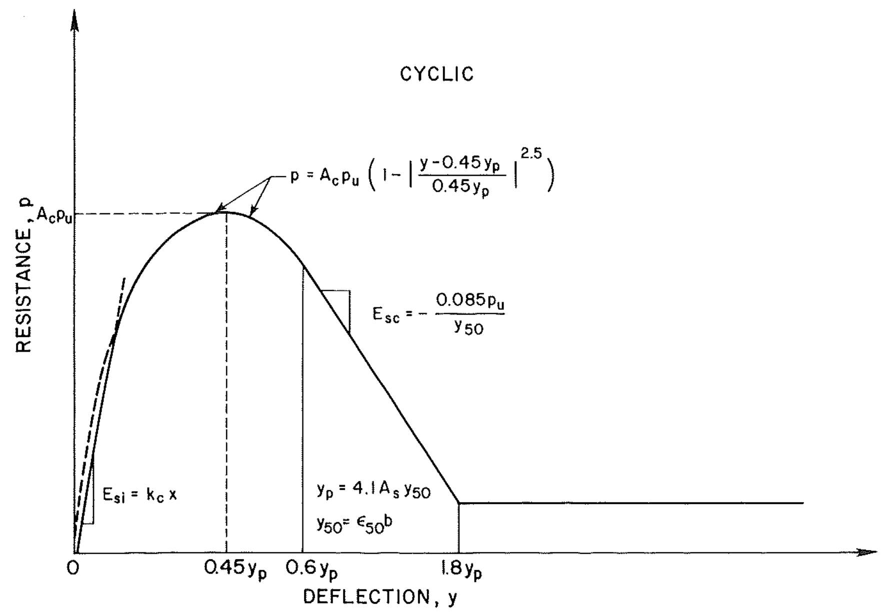

Fig. 7. Characteristic shape of p–y curve for cyclic loading in stiff clay below the water surface

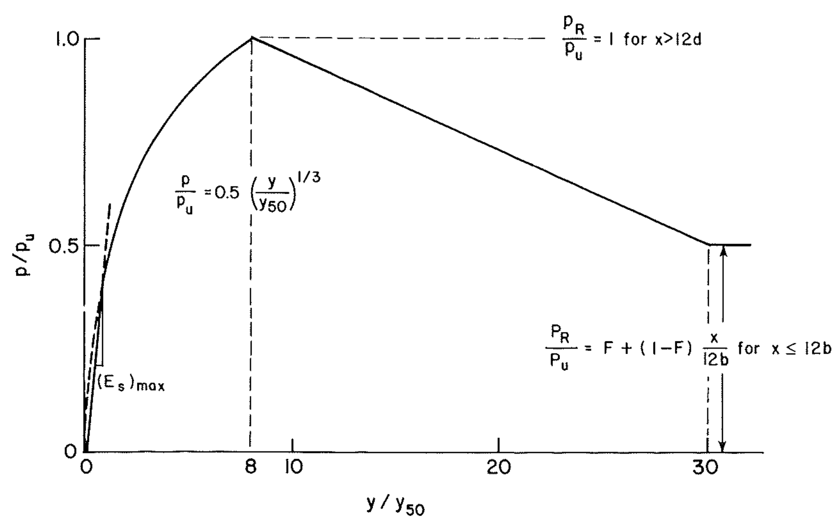

Fig. 8. Characteristic shape of p–y curve for unified clay criteria for short term static loading

Table 4. Values of N_p at the ground surface

Reference	N_p
Reese[8]	2
Hansen[9]	2.57
Thompson[10] (finite elements)	3.12
Matlock[4]	3
Reese et al.[7]	0.4

Table 5. Values of N_p at a depth of three pile diameters

Reference	N_p
Reese[8]	10.5
Hansen[9]	6.26
Thompson[10] (finite elements)	5.70 – 10.93
Matlock[4]	4.5
Reese et al.[7]	6.2

Table 6. Values of N_p at great depth

Reference	N_p at $x = 12b$	Limiting value of N_p
Reese[8]	–	12
Thompson[10] (block flow)	–	7 – 12
Hansen[9]	7.51	8.14
Thompson[10] (finite elements)	5.70 – 10.93	10.93
Matlock[4]	9	9
Reese et al.[7]	6.6	6.6

(i) Establish the final straight-line portion of the p–y curve,

$$p = 0.936 A_c p_u - 0.102 (p_u/y_{50}) y_p \tag{21}$$

Equation (21) should define the portion of the p–y curve from the point where $y = 1.8y_p$ and for all larger values of y (see following note).

17. Note: The step-by-step procedure is outlined, and Fig. 7 is drawn, as if there is an intersection between equations (11) and (19). However, there may be no intersection of those two equations and there may be no intersection of equation (11) with any of the other equations defining the p–y curve. If there is no intersection, the equation should be employed that gives the smallest value of p for any value of y.

18. The undrained shear strength of the soil and other soil properties should be obtained from appropriate laboratory or in situ tests.

DEVELOPMENT OF UNIFIED METHOD

19. The two sets of recommendations that have been presented for clays were used to compute the behaviour of the test piles, and the computed behaviour agreed well with that from the experiments. Furthermore, the recommendations were generalized as much as possible by using the principles of mechanics with the view of providing guidance for designers. However, designers have little or no guidance in solving problems where the properties of the clay are different than those at the experimental sites. In view of the need to have recommendations, at least in preliminary form, that can be employed to design piles under lateral loading in any clay soils, studies were made of the results of the two experimental programmes with a view to developing a unified approach. Those studies and their results are presented in the following sections.

20. A study was made of the ultimate soil resistance p_u that can be expected to develop against a pile that is subjected to lateral load. Two types of behaviour of the soil are postulated. Near the ground surface a wedge of soil is assumed to move up and out at the failure condition, and at depth the soil is assumed to flow around the pile at failure and a plane strain analysis can be employed. The value of p_u can be expressed in general form for failure near the ground surface as follows:

$$p_u = N_p (s_u)_{avg} b \tag{22}$$

The average value of the undrained shear strength is employed because of the assumption of the wedge type failure. At the depth where plane strain behaviour is assumed, the shear strength at the particular depth should be employed:

$$p_u = N_p s_u b \tag{23}$$

Table 4 shows values of N_p at the ground surface suggested by various investigators and Table 5 shows values suggested by the same authors at a depth of three pile diameters. The works cited in Tables 4 and 5 were studied and the major experimental studies[4, 7] were carefully considered. The following equations are proposed for the ultimate soil resistance near the ground surface:

$$p_u = \left\{2 + \frac{\bar{\gamma}}{(s_u)_{avg}} x + \frac{0.833}{b} x\right\} (s_u)_{avg} b \tag{24}$$

$$p_u = \left\{3 + \frac{0.5}{b} x\right\} s_u b \tag{25}$$

Equation (25) is similar to the one proposed by Matlock[4] except that the term involving submerged unit weight is omitted.

21. Equations (24) and (25) have some theoretical basis as indicated previously.[8] Table 6 gives values of N_p at great depth as recommended in the sources used for Tables 4 and 5. A value of N_p of 9 was adopted for the unified method, leading to the following equation for the ultimate resistance at great depth:

$$p_u = 9 s_u b \tag{26}$$

The smallest of the values of ultimate resistance computed by equations (24)–(26) should be employed.

22. The characteristic shape of the p–y curve for short term static loading is shown in Fig. 8. The initial portion of the curve is linear and is described by equation (27):

$$p = (E_s)_{max} y \tag{27}$$

The parameter $(E_s)_{max}$ is the limiting maximum value of soil modulus. When no other method is available, $(E_s)_{max}$ can be estimated using equation (28):

$$(E_s)_{max} = kx \tag{28}$$

Representative values for k are given in Table 7.

23. The curved portion of the p–y curve is described by equation (29):

$$p = 0.5 p_u (y/y_{50})^{1/3} \tag{29}$$

Equation (29) is identical to the equation recommended by

Table 7. Representative values for k for unified criteria

s_u, kPa	k, MN/m^3
12 – 25	8
25 – 50	27
50 – 100	80
100 – 200	270
200 – 400	800

Table 8. Representative values for ϵ_{50} for unified criteria

s_u, kPa	ϵ_{50}
12 – 25	0.02
25 – 50	0.01
50 – 100	0.007
100 – 200	0.005
200 – 400	0.004

Matlock[4] to define the soil resistance for the initial portion of the p–y curve.

24. The equation for computing y_{50} is

$$y_{50} = A \epsilon_{50} b \tag{30}$$

Values of ϵ_{50} may be taken from Table 8. The method for estimating A is discussed later.

25. The soil resistance after large deformation is given by equations (31) and (32). The smaller of the values computed by the two equations should be employed:

$$p_R = p_u \left\{ F + (1-F) \frac{x}{12b} \right\} \text{for } x < 12b \tag{31}$$

$$p_R = p_u \qquad \text{for } x > 12b \tag{32}$$

The parameter F is a function of the stress–strain characteristics of the soil and is discussed later. The selection of $30y_{50}$, the deflexion at which the residual resistance is reached, and the increase of p_R/p_u with depth are arbitrary. However, the use of the shape shown in Fig. 8 for the residual portion of the curve gives good agreement between the measured and computed values for experiments, as shown later.

26. The characteristic shape of the p–y curve for cyclic loading is shown in Fig. 9. The decrease in the soil resistance with depth due to cyclic loading is consistent with the recommendation made by Matlock.[4] The recommended shape of the cyclic p–y curve is completely empirical. However, its use does give satisfactory agreement between measured and computed values for full-scale experiments, as shown below.

27. Equations (30) and (31) for defining the p–y curves contain the coefficients A and F. These were determined empirically from results of load tests at Sabine and Manor and are given in Table 9 (where O_R is overconsolidation ratio, S_t is sensitivity, w_L is liquid limit, PI is plasticity index, and LI is liquidity index). The recommended procedure for estimating A and F for other clays is given below.

(a) Determine as many of the following properties of the clay as possible: s_u, ϵ_{50}, w_L, PI, LI, failure strain from stress–strain curve, overconsolidation ratio, degree of saturation, degree of fissuring, ratio of residual to peak shear strength.

(b) Compare the properties of the soil in question with the properties of the Sabine and Manor clays listed in Table 9.

(c) If the properties are similar to either the Sabine or Manor clay properties, use A and F for the similar clay. If the properties are not similar to either, the engineer should estimate A and F using his judgement with Table 9 as a guide.

28. The shapes of the p–y curves for the unified method (Figs 8 and 9) are based on the assumption that there is an intersection between equations (27) and (29). If that intersection does not occur, the p–y curve is defined by equation (27) until there is an intersection between equation (27) and the curves defining the p–y curves at greater pile deflexions.

Table 9. Curve parameters for unified criteria

Site	Sabine River	Manor
Clay description	Inorganic, intact $(s_u)_{avg} = 15$ kPa $\epsilon_{50} = 0.007$ $O_R \approx 1$ $S_t \approx 2$ $w_L = 92$ PI = 68 LI = 1	Inorganic, very fissured $(s_u)_{avg} \approx 115$ kPa $\epsilon_{50} = 0.005$ $O_R > 10$ $S_t \approx 1$ $w_L = 77$ PI = 60 LI ≈ 0.2
A	2.5	0.35
F	1.0	0.5

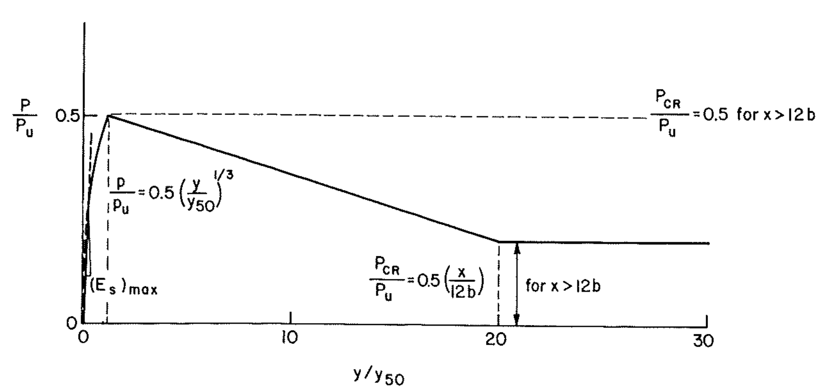

Fig. 9. Characteristic shape of p–y curve for unified clay criteria for cyclic loading

COMPARISON OF RESULTS FROM ANALYSES WITH THOSE FROM EXPERIMENTS

Lake Austin

29. The Lake Austin tests and others in this section were analysed using both the unified criteria and the criteria previously proposed.[4,7] The parameters A and F for the unified criteria were chosen as 2.5 and 1.0 respectively, based on an average shear strength of 38 kPa as measured by the vane test. The Lake Austin clay is inorganic and slightly fissured and is classified as a CH. It has a liquid limit of 64, a plasticity index of 41, a liquidity index of 0.5, an overconsolidation ratio of about 4, and a sensitivity of about 3. The water table was above the ground surface and the submerged unit weight of the soil was 800 kg/m³. The value of ϵ_{50} was 0.012.

30. The pile head was free to rotate. The loadings were short term static and cyclic. The maximum moments computed by the unified criteria are in good agreement with the measured values, as shown in Figs 10 and 11. In general, the results using the unified criteria agree slightly better with experimental results than do the results using the Matlock criteria.

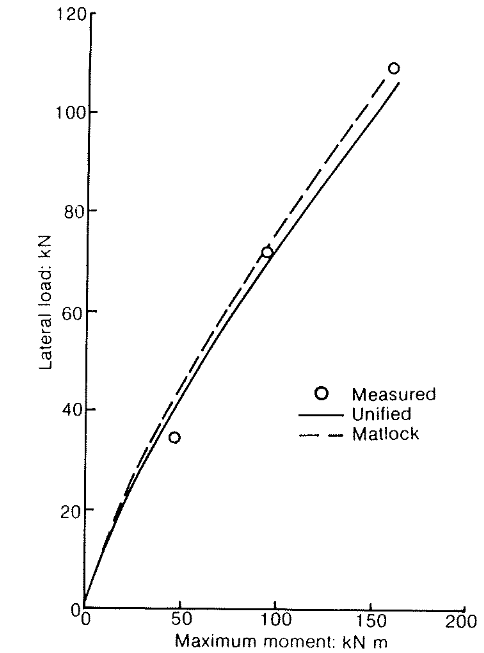

Fig. 10. Comparison of measured and computed maximum moments for Lake Austin for short term static loading

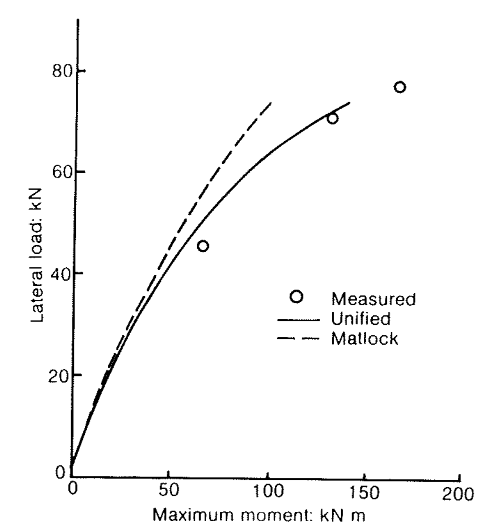

Fig. 11. Comparison of measured and computed maximum moments for Lake Austin for cyclic loading

Sabine

31. The Sabine tests were performed at a site where the clays were described as a slightly overconsolidated marine deposit. The properties of the clay are shown in Table 9. As indicated, the factors A and F were selected as 2.5 and 1.0, respectively.

32. The water table was above the ground surface, the pile head was free to rotate, and the loadings that are analysed in this Paper were short term static and cyclic. The

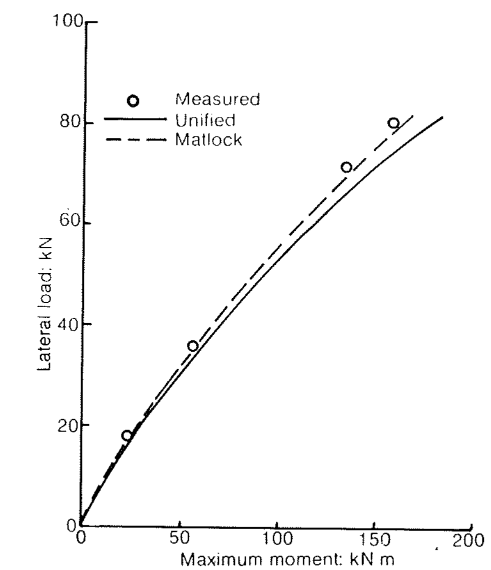

Fig. 12. Comparison of measured and computed maximum moments for Sabine for short term static loading

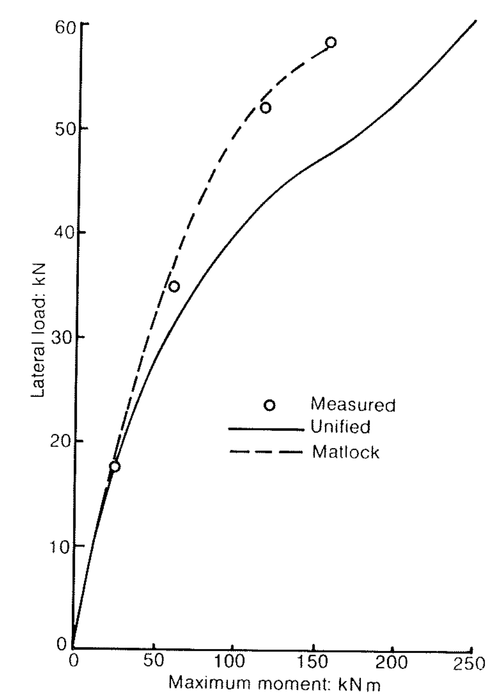

Fig. 13. Comparison of measured and computed maximum moments for Sabine for cyclic loading

results of computations using the unified criteria and the Matlock criteria are compared with experimental results in Figs 12 and 13. Agreements are good in all cases for loads of relatively low magnitude. At the higher loads for the short term static loading, the Matlock criteria give somewhat better agreement with the experiment than does the unified method; and considerably better agreement at the higher loads for the cyclic loading case.

Manor

33. The clay at Manor is highly overconsolidated, inorganic and very fissured. The properties of the clay are given in Table 9. As indicated, the factors A and F were selected as 0.35 and 0.5, respectively.

34. The water table was above the ground surface, the pile head was free to rotate, and the loadings were short term static and cyclic. The results of computations using the unified criteria and the Reese et al. criteria are compared with experimental results in Figs 14 and 15. As can be seen, excellent agreement was obtained in all instances. It is not shown here, but excellent agreement was obtained between computed groundline deflexions using both methods and the deflexions from the experiment.

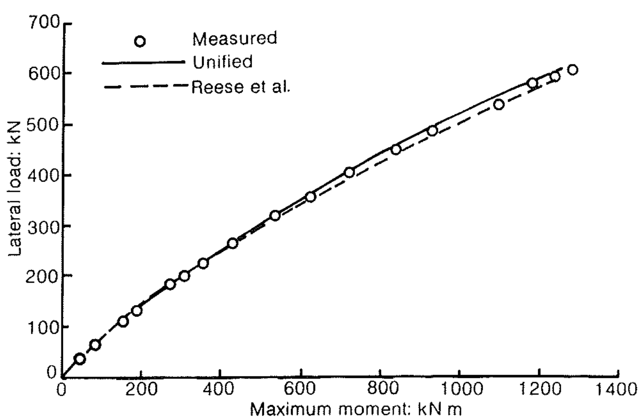

Fig. 14. Comparison of measured and computed maximum moments for Manor for short term static loading

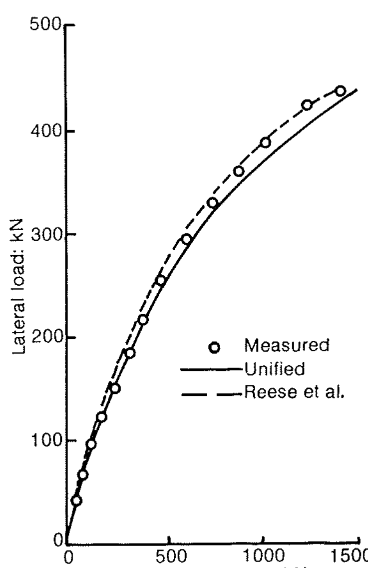

Fig. 15. Comparison of measured and computed maximum moments for Manor for cyclic loading

San Francisco Bay mud

35. Short term static tests, reported by Gill,[11] were performed on steel pipe piles of four different diameters whose properties are given in Table 10. The pile head was free to rotate. The load was applied 800 mm above the ground surface. Groundline deflexions and slopes were measured, but no data were given on slopes. The distribution of shear strength used in the analysis was measured with an in situ vane, and is given in Fig. 16. The soil at the site is described as an insensitive, gray, slightly organic, silty clay and is classified as a CH in the unified classification system. The liquid limit is 71, the plasticity index is 29. For purposes of computation ϵ_{50} was estimated as having a value of 0.01. The submerged unit weight was estimated as 800 kg/m^3.

36. The test site was flooded several days before the test, the water level being raised to approximately 30 mm above the ground surface. The shear strength in Fig. 16 was measured after the strength had stabilized after flooding.

37. The tests in bay mud were analysed using the unified criteria. The parameters A and F were chosen as 2.5 and 1.0, respectively, because the bay mud was felt to be similar to the Sabine clay, based on the limited soil data. The computed groundline deflexions are less than the measured values in all cases, as shown in Figs 17 and 18. The most probable source of error is in the value of the coefficient A. A larger value of A would lead to a better agreement, and is probably justified.

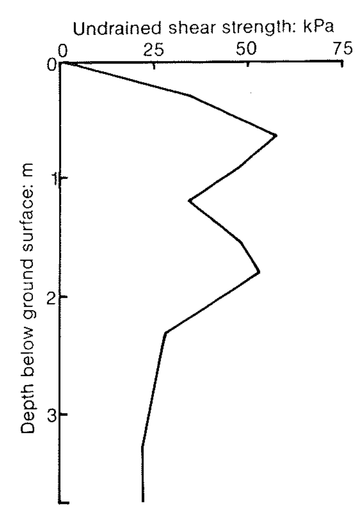

Fig. 16. Distribution of shear strength used for bay mud

Table 10. Pile properties for tests in bay mud

Pile	Diameter, b, mm	Bending stiffness, EI, kN m^2	Penetration, m
P1	114	6.23×10^5	5.55
P2	219	5.26×10^6	6.22
P3	324	3.12×10^7	5.09
P4	406	4.84×10^7	8.14

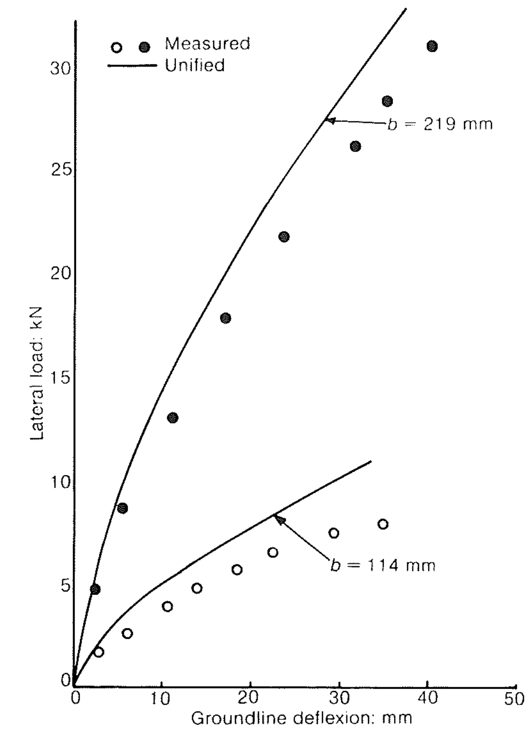

Fig. 17. Comparison of measured and computed groundline deflexion for piles P1 and P2 in bay mud

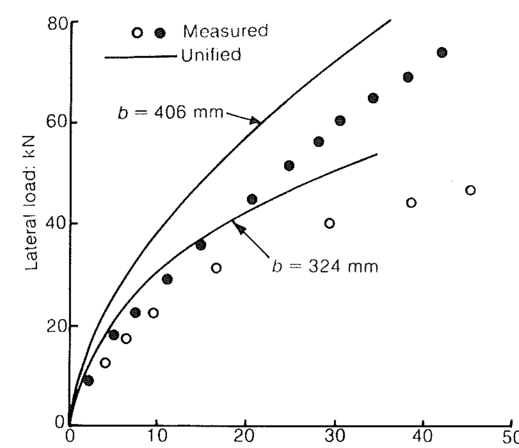

Fig. 18. Comparison of measured and computed groundline deflexions for piles P3 and P4 in bay mud

El Centro clay

38. Short term static tests, reported by Gill and Demars,[12] were performed on steel pipe piles of four different diameters whose properties are given in Table 11. The pile head was free to rotate. The load was applied at 810 mm above the ground surface. Groundline deflexions and slopes were measured. The distribution of shear strength used in the analysis was measured with an in situ vane, and is given in Fig. 19. The soil at the site is described as a silty clay and a clayey silt and is classified as a ML–CL in the unified classification system. The liquid limit is 32 and the

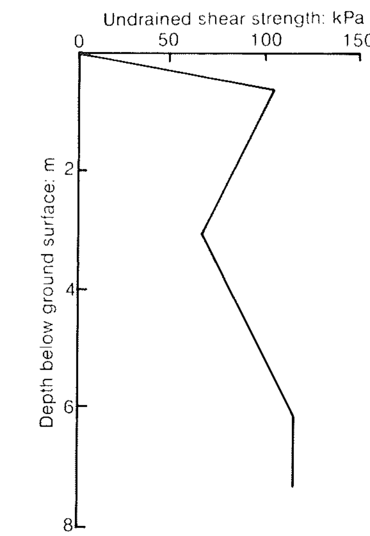

Fig. 19. Distribution of shear strength used for El Centro clay

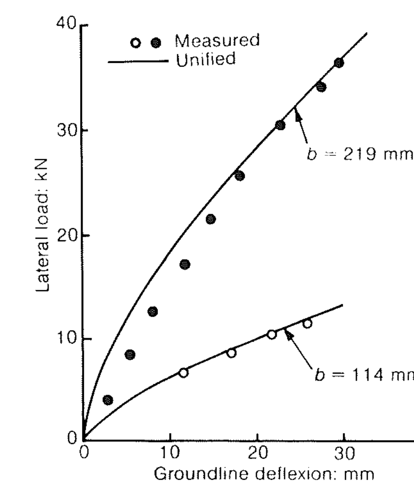

Fig. 20. Comparison of measured and computed groundline deflexions for piles P1 and P2 in El Centro clay

Table 11. Pile properties for tests at El Centro

Pile	Diameter, b, mm	Bending stiffness, EI, kN m^2	Penetration, m
P1	114	6.49×10^5	3.66
P2	219	4.97×10^6	5.18
P3	324	2.41×10^7	6.71
P4	406	4.84×10^7	8.23

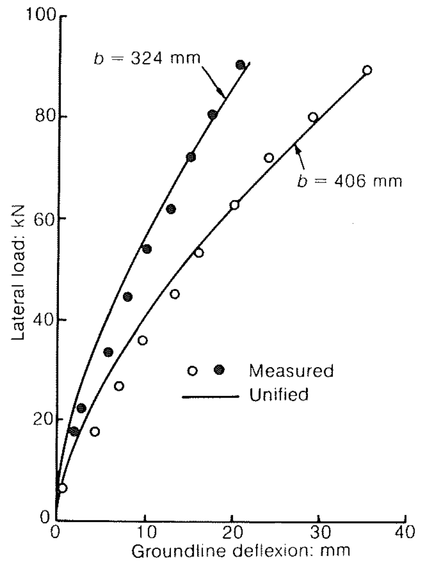

Fig. 21. Comparison of measured and computed groundline deflexions for piles P3 and P4 in El Centro clay

plasticity index is 10. For purposes of computation, ϵ_{50} was estimated as having a value of 0.01. The submerged unit weight was estimated as 800 kg/m^3.

39. The test site was flooded, the same as for the bay mud site, and the strength given in Fig. 19 was measured after the strength had stabilized after flooding.

40. The tests at El Centro were analysed using the unified criteria. The parameters A and F were chosen as 2.5 and 1.0, respectively, because the El Centro clay was felt to be similar to the Sabine clay, based on the limited soil data. The computed groundline deflexions are in good agreement with the measured values, for all four pile sizes, as shown in Figs 20 and 21.

CONCLUDING COMMENTS

41. The ability to predict the behaviour of piles under lateral loading is dependent on being able to derive curves giving the soil response (p–y curves). Two methods of predicting soil response curves for submerged clays have been published: Matlock[4] and Reese et al.[7] Results from the experimental programmes on which the methods of Matlock and Reese et al. were based were reanalysed and a single method, the unified method, was derived. The computed results employing the unified method agreed well with the experimental results reported by Matlock and Reese et al., and also agreed reasonably well with results from other experiments.

42. While the unified method presents a single and a somewhat simpler approach for predicting p–y curves for submerged clays, both under short term static and cyclic loadings, the method involves the selection of two empirical parameters with only a minor amount of guidance from experiments and none from theory. It is plain that additional experiments employing full-sized, instrumented piles in a variety of submerged clays are sorely needed.

43. In spite of the lack of full validation of the methods of predicting p–y curves, the approach described herein is believed to be the best currently available. It is hoped that the unified method presented here can be the vehicle to correlate the results from additional experiments into a single set of p–y criteria for submerged clays.

ACKNOWLEDGEMENTS

44. Most of the work described in this Paper was supported by a grant from the National Science Foundation, ENG. 74-19444. McClelland Engineers also provided financial assistance. The support of the sponsors is gratefully acknowledged.

REFERENCES

1. HETENYI M. Beams on elastic foundation. University of Michigan Press, Ann Arbor, Michigan, 1946.
2. REESE L. C. and MANOLIU I. Analysis of laterally loaded piles by computer. Buletinul Stiintific Al Institutului De Constructii Bucuresti, 1973, XVI, No. 1, 35–70.
3. MATLOCK H. and REESE L. C. Foundations analysis of offshore pile supported structures. Proc. 5th Int. Conf. International Society of Soil Mechanics and Foundation Engineering, Paris, 1961, 2, 91–97.
4. MATLOCK H. Correlations for design of laterally loaded piles in soft clay. Proc. 2nd Annual Offshore Technology Conf. Houston, Texas, 1970, 1, 577–594. Paper OTC 1204.
5. MATLOCK H. and RIPPERGER E. A. Measurements of soil pressure on a laterally loaded pile. Proc. Am. Soc. Test. Mater. 1958, 58, 1245–1259.
6. SKEMPTON A. W. The bearing capacity of clays. Proc. Building Research Congress, Division I, London, 1951, Part III, 180–189.
7. REESE L. C. et al. Field testing and analysis of laterally loaded piles in stiff clay. Proc. 7th Offshore Technology Conf. Houston, Texas, 1975, 2, 473–483, Paper OTC 2312.
8. REESE L. C. Discussion of soil modulus for laterally loaded piles by Bramlette McClelland and John A. Focht, Jr. Trans. Am. Soc. Civ. Engrs, 1958, 123, 1071–1074.
9. HANSEN J. B. The ultimate resistance of rigid piles against transversal forces. The Danish Geotechnical Institute, Copenhagen, 1961, bulletin 12, 5–9.
10. THOMPSON G. R. Application of the finite element method to the development of p–y curves for saturated clays. Master's thesis, The University of Texas, Austin, 1977.
11. GILL H. L. Soil behavior around laterally loaded piles. Naval Civil Engineering Laboratory, Port Hueneme, California, 1968, report R–670.
12. GILL H. L. and DEMARS K. R. Displacement of laterally loaded structures in nonlinearly responsive soil. Naval Civil Engineering Laboratory, Port Hueneme, California, 1970, report R–760.